

Supporting Information

Efficient Photocatalytic Hydrogen Production in Water using a Cobalt(III) Tetraaza-macrocyclic Catalyst. Electrochemical Generation of the Low-valent Co(I) Species and its Reactivity toward Proton Reduction

Siddhartha Varma,^a Carmen E. Castillo,^a Thibaut Stoll,^a Jérôme Fortage,^a Allan G. Blackman,^b Florian Molton,^a Alain Deronzier^{a*} and Marie-Noëlle Collomb^{a*}

^aUniversité Joseph Fourier Grenoble 1 / CNRS, Département de Chimie Moléculaire, UMR 5250, Institut de Chimie Moléculaire de Grenoble, FR-CNRS-2607, Laboratoire de Chimie Inorganique Rédox, BP 53, 38041 Grenoble Cedex 9, France

^bDepartment of Chemistry, University of Otago, P.O. Box 56, Dunedin, New Zealand

Email: marie-noelle.collomb@ujf-grenoble.fr, alain.deronzier@ujf-grenoble.fr

Materials: 2,2'-bipyridine (bpy, 99%, Aldrich), 4,4'-dimethyl-2,2'-bipyridine (dmbpy, 99%, Fluka), diacetylmonoxime (99%, Alfa Aesar), 1,3-diaminopropane (+99%, Aldrich), CoCl₂·6H₂O (98%, Aldrich), CoBr₂·xH₂O (Aldrich), RhCl₃·xH₂O (38% Rh, Acros), [Ru(bpy)₃]Cl₂ (**PS1**) (99%, Aldrich), L-ascorbic acid (H₂A, 99%, Acros), sodium L-ascorbate (NaHA, 99%, Acros), acetonitrile (CH₃CN, Rathburn, HPLC grade), tetra-*n*-butyl-ammonium perchlorate ([Bu₄N]ClO₄, Fluka) and reference gas (1% and 5% H₂ in N₂, Air Liquide) were purchased from commercial suppliers. All reagents and solvents were used as received. Purification of water (15.0 MΩ.cm, 24°C) was performed with a milli-Q system (Purelab option, Elga).

Synthesis of the complexes:

[Co(CR)Cl₂](ClO₄) (**Cat1**). 2,6-diacetyl-pyridine (686 mg, 4.2 mmol) was dissolved in ethanol (6.3 mL) and kept at 40°C under argon. CoCl₂·6H₂O (1 g, 4.2 mmol) and water (4.2 mL) were added and the mixture was stirred at 55°C to dissolve the salt, giving a purple solution. The reaction mixture was warmed at 75°C and 3,3'-diaminodipropylamine (0.59 mL, 4.2 mmol) was added. The colour turned to dark blue and the solution became cloudy on addition of the amine. Glacial acetic acid (0.17 mL) was added to solubilise and clarify the solution which was stirred at 75°C for 5 hours under argon. At this time, the condensation was judged to be complete and concentrated HCl aqueous solution (0.39 mL, 4.62 mmol, 37 %) was added, after which the solution turned to an orange/brown colour. The mixture was aerated for about 6 hours affording a green solution. The volume was reduced on the rotary evaporator until 1 mL water was left. Cold ethanol (7 mL) at -8°C was added slowly and the product [Co^{III}(CR)Cl₂]Cl precipitated as green microcrystals. The green crystals were filtered off and washed with cold ethanol. The product was recrystallized from a mixture of water and cold ethanol (-8°C) and dried under vacuum (692 mg, 39 %). [Co^{III}(CR)Cl₂]Cl was dissolved in water (5 mL) and an aqueous saturated solution of LiClO₄ was added dropwise to yield [Co^{III}(CR)Cl₂](ClO₄) as a green precipitate. The product was filtered off, recrystallized in hot water, filtered off a second time and dried under vacuum, affording green crystals (630 mg, 31%). Anal. Calcd for C₁₅H₂₂Cl₃CoN₄O₄: C, 36.94; H, 4.55; N, 11.49; Cl, 21.81. Found: C, 36.89; H, 4.53; N, 11.42; Cl, 21.62. ¹H NMR (400 MHz, CD₃CN) δ = 8.55 (t, J = 8.0 Hz, 1H), 8.35 (d, J = 8.0 Hz, 2H), 4.00 (br d, J = 15.6 Hz, 2H), 3.56 (br t, J = 14.8 Hz, 2H), 3.31 (q, J = 12.0 and 12.0 Hz, 2H), 2.94-2.85 (m, 2H), 2.81 (s, 6H), 2.29 (br d, J = 15.6 Hz, 2H), 2.12-2.08 (m, 2H).

[Co(CR)(H₂O)₂](ClO₄)₃. Two equivalents of Ag(ClO₄)·H₂O (327 mg, 1.45 mmol) were added as a solid to a suspension of [Co^{III}(CR)Cl₂](ClO₄) (354 mg, 0.726 mmol) in water (10 mL). The reaction mixture was stirred for 2h in the dark. The crude mixture was filtered through a celite pad to remove AgCl. The filtrate was concentrated under vacuum to 5 mL and perchloric acid (2 mL, 70% in water) was added dropwise. The solution was stirred at room temperature over 20 hours, affording brown

microcrystals of $[\text{Co}^{\text{III}}(\text{CR})(\text{H}_2\text{O})_2](\text{ClO}_4)_3$. The product was filtered off, washed with Et_2O and dried under vacuum (293 mg, 62%). ^1H NMR (400 MHz, D_2O) δ = 8.87 (t, J = 8.4 Hz, 1H), 8.71 (d, J = 8.4 Hz, 2H), 4.21 (br d, J = 16.4 Hz, 2H), 3.80 (br t, J = 14.4 Hz, 2H), 3.20–3.11 (m, 4H), 3.07 (s, 6H), 2.61 (br d, J = 15.6 Hz, 2H), 2.27–2.15 (m, 2H).

Determination of the turnover number (TON): The number of moles (n_{H_2}) and the volume (V_{H_2}) of hydrogen produced was calculated according to the following Equations S1 and S2, respectively:

$$n_{\text{H}_2}(\text{mol}) = \frac{\text{Detected peak area}}{\text{Calibration peak area}} \times 0.01 \times \frac{\text{Headspace volume [L]}}{24.5 \text{ [L mol}^{-1}\text{]}} \quad (\text{S1})$$

$$V_{\text{H}_2}(\text{L}) = \frac{\text{Detected peak area}}{\text{Calibration peak area}} \times 0.01 \times \text{Headspace volume [L]} \quad (\text{S2})$$

where 0.01 is the reference percentage of H_2 in N_2 (corresponding to 1% of H_2 in N_2) which is linked to the calibration peak area, 24.5 Lmol^{-1} is the molar volume of an ideal gas at a temperature of 298.15 K and pressure of 101325 Pa. For all experiments, the overpressure in the schlenk tube (headspace volume 175 mL) due to the hydrogen produced was regarded as small, since the total amount of hydrogen produced did not exceed 12.5 mL.

The turnover number related to the catalyst (TON_{Cat}) was calculated according to the following Equation S3:

$$\text{TON}_{\text{Cat}} = \frac{n_{\text{H}_2}}{n_{\text{Cat}}} \quad (\text{S3})$$

where n_{H_2} is the number of moles of hydrogen produced, and n_{Cat} is the number of moles of catalyst initially present in solution. We consider that one mole of catalyst gives 1 mole of H_2 .

The turnover number related to the photosensitizer (TON_{PS}) was calculated according to the following Equation S4:

$$\text{TON}_{\text{PS}} = \frac{2 \times n_{\text{H}_2}}{n_{\text{PS}}} \quad (\text{S4})$$

where n_{PS} is the number of moles of photosensitizer initially present in solution. We consider that two moles of photosensitizer give 1 mole of H_2 .

For all experiments, the TON's were calculated after the H_2 evolution stopped (between 5 and 25 hours).

Mercury poisoning test for photocatalytic experiments: To exclude the formation of colloidal cobalt that can be catalytically active for the reduction of protons into hydrogen, a mercury poisoning test was performed. Indeed mercury is known to poison or inhibit the activity of metal catalysts including colloids¹ and forms an amalgam with Co.² This test was performed by adding a drop of mercury in an aqueous solution containing **PS1** (5×10^{-4} M), **Cat1** (1×10^{-4} M), H_2A (0.55 M) and NaHA (0.55 M) at pH 4.0. This mixture was stirred and degassed by nitrogen bubbling during 45 min. Then the sample was irradiated under vigorous stirring and the H_2 production analysed under the same conditions as the classical photocatalysis experiment. The presence of a large excess of mercury has no significant effect on the catalytic activity of **Cat1**, clearly indicating that no significant colloid formation occurs during the photocatalytic H_2 production.

Generation of hydrogen by addition of protons into electrogenerated solution of $[\text{Co}^{\text{I}}(\text{CR})]^+$:

A 1 mM solution of $[\text{Co}^{\text{I}}(\text{CR})]^+$ (20 mL) in $\text{CH}_3\text{CN} + 0.1$ M Bu_4NClO_4 was prepared by an exhaustive electrolysis at $E = -1.10$ V of a 1 mM solution of $[\text{Co}^{\text{III}}(\text{CR})\text{Cl}_2]^+$ (20 μmol) under an inert atmosphere (glove box). The resulting solution was divided into two solutions of 5 and 15 mL, that contained

respectively 5 and 15 μmol of Co^{I} . The 5 mL solution was transferred into a round bottom flask closed with a septum (total volume = 17 mL, headspace volume = 12 mL).

One equivalent of *p*-cyano-anilinium tetrafluoroborate was then reacted with the 5 and 15 mL Co^{I} solutions by addition, under stirring, of 36.5 μL and 109 μL of a 137 mM CH_3CN solution of this acid respectively. A color change of the Co^{I} solutions from colorless to orange within about 4 seconds was observed. Analysis of the 15 mL solution by UV-vis absorption spectroscopy (Figure 5) and CV (Figure S9) evidenced the quantitative formation of the Co^{II} species. Analysis of the gas mixture in the headspace of the flask containing the 5 mL solution by gas chromatography shows that 2.1 μmol of H_2 is produced, corresponding to 0.42 equivalent per initial Co^{I} species.

A similar procedure was used for the reaction of 2 equivalents of *p*-cyano-anilinium tetrafluoroborate with Co^{I} except that 250 μL (10 μmol of acid) and 750 μL (30 μmol of acid) of a 40 mM of the CH_3CN solution of *p*-cyano-anilinium tetrafluoroborate were added to the 5 mL and 15 mL of Co^{I} CH_3CN solutions, respectively (Figures S9-S10). Analysis of the gas mixture in the headspace of the flask containing the 5 mL solution by gas chromatography shows that 2.16 μmol of H_2 is produced, corresponding to 0.43 equivalent per initial Co^{I} species.

For the reaction of Co^{I} with 20 equivalents of *p*-cyano-anilinium tetrafluorobororate, a 160 mM CH_3CN solution of this acid was prepared. 625 μL (100 μmol of acid) and 1.9 mL (300 μmol of acid) of a 160 mM of the CH_3CN solution of *p*-cyano-anilinium tetrafluoroborate were added to the 5 mL (5 μmol) and 15 mL (15 μmol) of $\text{CH}_3\text{CN} + 0.1 \text{ M } \text{Bu}_4\text{NClO}_4$ solutions of Co^{I} , respectively (Figures S9-S10). Analysis of the gas mixture in the headspace of the flask containing the 5 mL solution by gas chromatography shows that 1.95 μmol of H_2 is produced, corresponding to 0.39 equivalent per initial Co^{I} species.

Table S1. Various concentrations of ascorbic acid (H_2A) and sodium ascorbate (NaHA) at different pH in aqueous solution.

pH	Concentration of H_2A ([mol L ⁻¹])	Concentration of NaHA ([mol L ⁻¹])
2.0	1.09	0.01
3.0	1.00	0.1
3.6	0.79	0.31
3.8	0.67	0.43
4.0	0.55	0.55
4.25	0.40	0.70
4.5	0.26	0.84
5.0	0.10	1.00
5.5	0.03	1.07
6.0	0.01	1.09

Table S2. Electrochemical potentials *versus* the Saturated Calomel Electrode (SCE) of the catalysts used in this work, **PS1** and HA⁻. $E_{1/2} = (E_{p_a} + E_{p_c})/2$. Potentials referred vs SCE can be converted to the Ag/0.01 M AgNO₃ in CH₃CN by subtracting 298 mV.

Compound	Solvent (pH)	E_{ox}	E_{red1} (ΔE_p)	E_{red2} (ΔE_p)
[Co(CR)Cl ₂]ClO ₄ (Cat1) ³	CH ₃ CN	-	$E_{1/2} = -0.10$ V (94 mV) (Co ^{III} /Co ^{II})	$E_{1/2} = -0.57$ V (87mV) (Co ^{II} /Co ^I)
[Co(CR)Cl ₂]ClO ₄ (Cat1) ³	H ₂ O	-	$E_{1/2} = +0.23$ V (128 mV) (Co ^{III} /Co ^{II})	$E_{1/2} = -0.85$ V (69 mV) (Co ^{II} /Co ^I)
[Co(CR)(H ₂ O) ₂](ClO ₄) ₃ ^{This work}	CH ₃ CN	-	$E_{1/2} = +0.62$ V (500 mV) (Co ^{III} /Co ^{II})	$E_{1/2} = -0.50$ V (80 mV) (Co ^{II} /Co ^I)
[Co(dmbpy) ₃]Cl ₃ (Cat3) ⁴	H ₂ O (9.6)	-	$E_{1/2} = -0.09$ V (Co ^{III} /Co ^{II})	$E_{1/2} = -1.28$ V (Co ^{II} /Co ^I)
[Co{(DO)(DOH)pn}Br ₂] (Cat2) ⁵	CH ₃ CN	-	$E_{1/2} = -0.29$ V (Co ^{III} /Co ^{II})	$E_{1/2} = -0.74$ V (Co ^{II} /Co ^I)
[Rh(dmbpy) ₂ Cl ₂]Cl (Cat5) ⁶	H ₂ O (8.0)	-	$E_{p_c} = -0.79$ V (Rh ^{III} /Rh ^I) $E_{p_a} = -0.25$ V (Rh ^I /Rh ^{III})	
[Ru(bpy) ₃]Cl ₂ (PS1) ^{7,8}	H ₂ O (7.0)	$E_{1/2} = +1.03$ V (Ru ^{III} /Ru ^{II})	$E_{1/2} = -1.50$ V (bpy/bpy ⁻ also denoted Ru ^{II} /Ru ^I)	
[Ru(bpy) ₃]Cl ₂ * (PS1*) ^{[a]7,8}	H ₂ O (7.0)	-1.07 V (Ru ^{III} /Ru ^{II*})	+0.60 V (Ru ^{II*} /Ru ^I)	
HA ⁻ (sodium ascorbate salt) ⁹	H ₂ O (4.0)	+0.30 V		

[a] Oxidation and reduction potentials of the excited state of **PS1** (marked by *) estimated by using the formula : $E_{1/2}(\text{Ru}^{\text{III}}/\text{Ru}^{\text{II}*}) = E_{1/2}(\text{Ru}^{\text{III}}/\text{Ru}^{\text{II}}) - E_{0,0}$ and $E_{1/2}(\text{Ru}^{\text{II}*}/\text{Ru}^{\text{I}}) = E_{1/2}(\text{Ru}^{\text{II}}/\text{Ru}^{\text{I}}) + E_{0,0}$, where $E_{0,0}$ is the energy level of the relaxed triplet excited state (³MLCT) of [Ru(bpy)₃]Cl₂ in acetonitrile, which is equal to 2.1 eV.

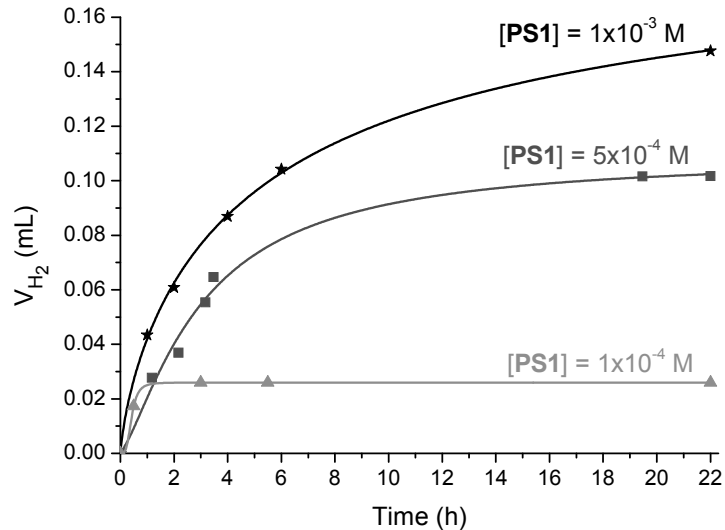


Figure S1. Photocatalytic hydrogen production (V_{H_2}) as a function of time from a deaerated water solution (5 mL) at pH 4.0 containing **PS1** at various concentrations ($1 \times 10^{-3} M$, $5 \times 10^{-4} M$ or $1 \times 10^{-4} M$), H₂A (0.55 M) and NaHA (0.55 M) under 400 - 700 nm irradiation.

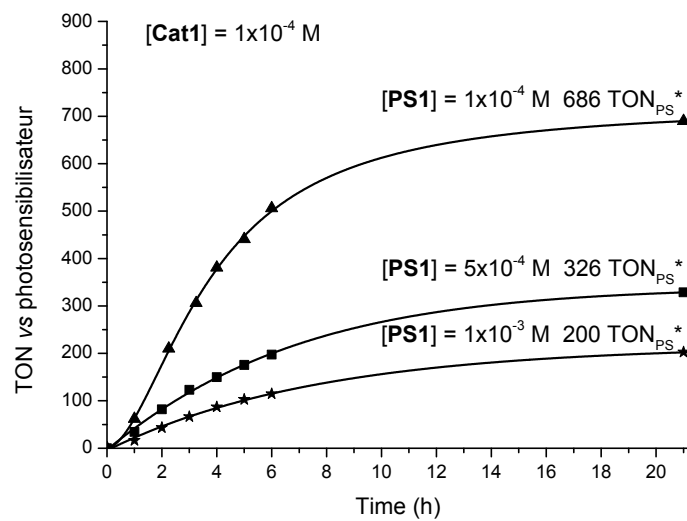


Figure S2. Photocatalytic hydrogen production (TON_{PS}) as a function of time from a deaerated aqueous solution (5 mL) of H₂A (0.55 M) and NaHA (0.55 M) at pH 4.0 under 400 - 700 nm irradiation in the presence of **Cat1** ($1 \times 10^{-4} M$) and **PS1** at various concentrations.

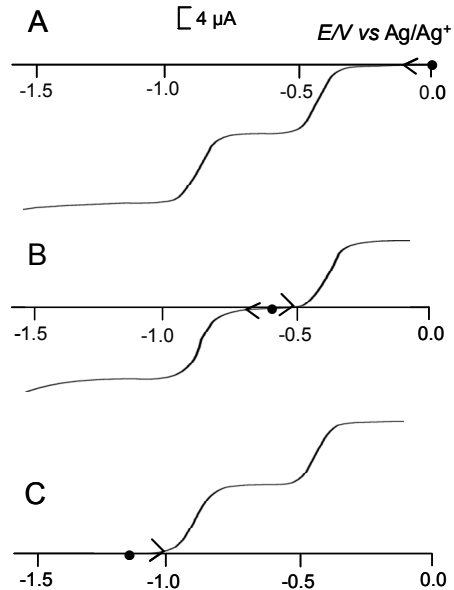


Figure S3. Voltammograms at a Rotating Disk Electrode (glassy carbon) at $\omega = 600 \text{ tr min}^{-1}$ ($\nu = 10 \text{ mV s}^{-1}$) in $\text{CH}_3\text{CN} + 0.1 \text{ M } \text{Bu}_4\text{NClO}_4$ of a 1 mM solution of $[\text{Co}^{\text{III}}(\text{CR})\text{Cl}_2]^+$ (**Cat1**) (A), and after two successive exhaustive reductions at -0.69 V (B), and at -1.10 V vs Ag/Ag^+ (C), leading to the formation of Co^{II} and Co^{I} , respectively. Potentials referenced to Ag/AgNO_3 10 mM can be converted to Fc^+/Fc^0 by subtracting 87 mV

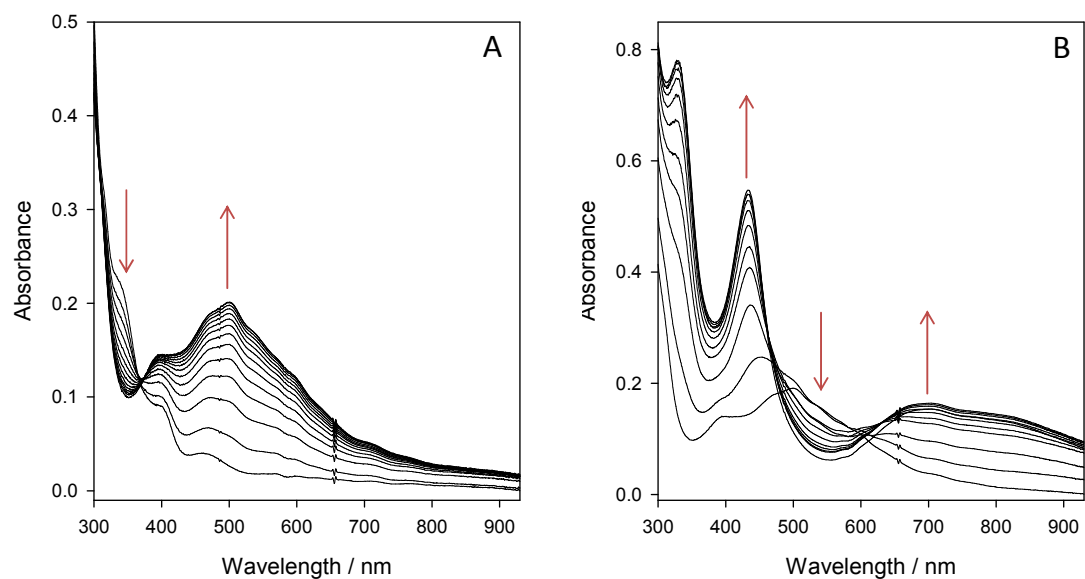


Figure S4. UV-visible absorption spectral changes in $\text{CH}_3\text{CN} + 0.1 \text{ M } \text{Bu}_4\text{NClO}_4$ of a 1 mM solution of **Cat1** during exhaustive electrolysis at -0.69 V (A), and during exhaustive electrolysis at -1.10 V vs Ag/Ag^+ (B) (formation of Co^{II} and Co^{I} , respectively), optical pathlength 1 mm .

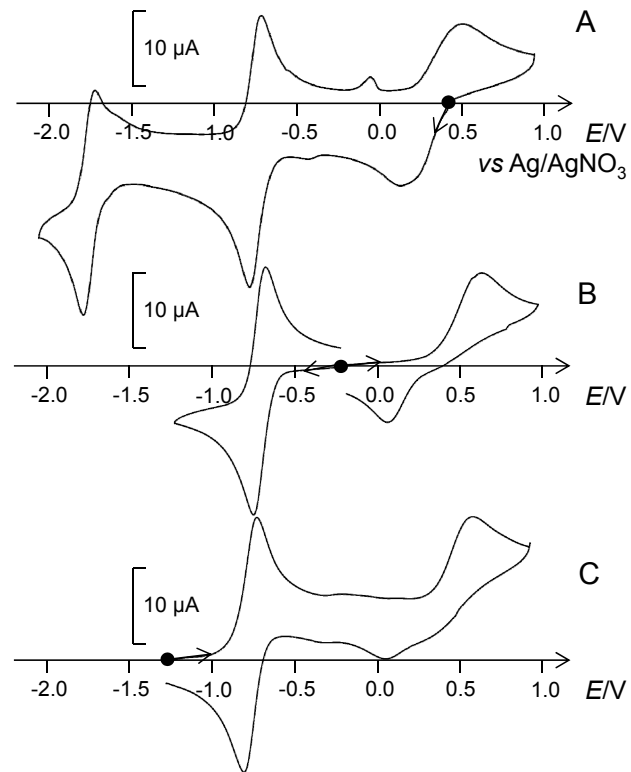


Figure S5. Cyclic voltammograms in $\text{CH}_3\text{CN} + 0.1 \text{ M } \text{Bu}_4\text{NClO}_4$ at a glassy carbon electrode ($v = 100 \text{ mV s}^{-1}$) of a 1 mM solution of $[\text{Co}^{\text{III}}(\text{CR})(\text{H}_2\text{O})_2]^+$ (A), and after two successive exhaustive reductions at -0.3 V (B) and at -1.33 V vs Ag/Ag^+ (C) (formation of Co^{II} and Co^{I} , respectively). Potentials referenced to Ag/AgNO_3 10 mM can be converted to Fc^+/Fc^0 by subtracting 87 mV .

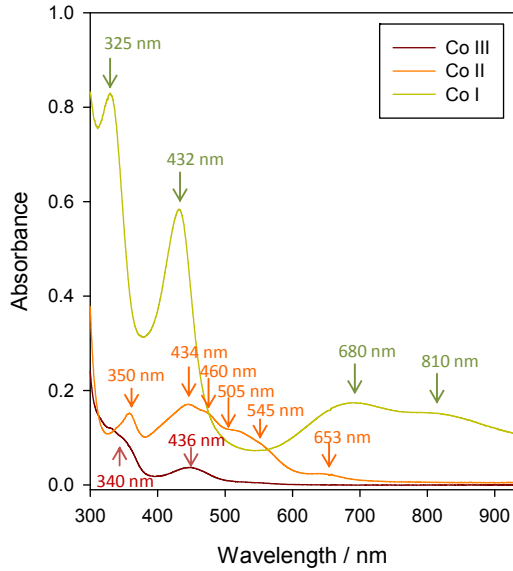


Figure S6. UV-visible absorption spectra in $\text{CH}_3\text{CN} + 0.1 \text{ M Bu}_4\text{NClO}_4$ of a 1 mM solution of $[\text{Co}^{\text{III}}(\text{CR})(\text{H}_2\text{O})_2]^+$ before (red) and after two exhaustive electrolyses at -0.30 V (orange) and -1.33 V vs Ag/Ag^+ (green) (formation of Co^{II} and Co^{I} , respectively), optical pathlength 1 mm.

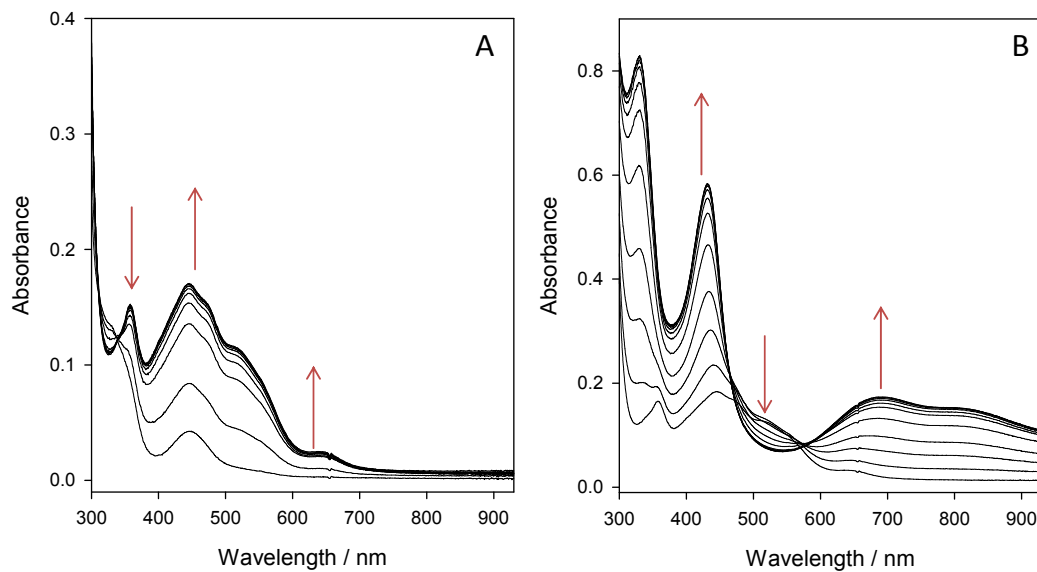


Figure S7. UV-visible absorption spectral changes in $\text{CH}_3\text{CN} + 0.1 \text{ M Bu}_4\text{NClO}_4$ of a 1 mM solution of $[\text{Co}^{\text{III}}(\text{CR})(\text{H}_2\text{O})_2]^+$ during exhaustive electrolysis at -0.30 V (A) and, during exhaustive electrolysis at -1.33 V vs Ag/Ag^+ (B), optical pathlength 1 mm.

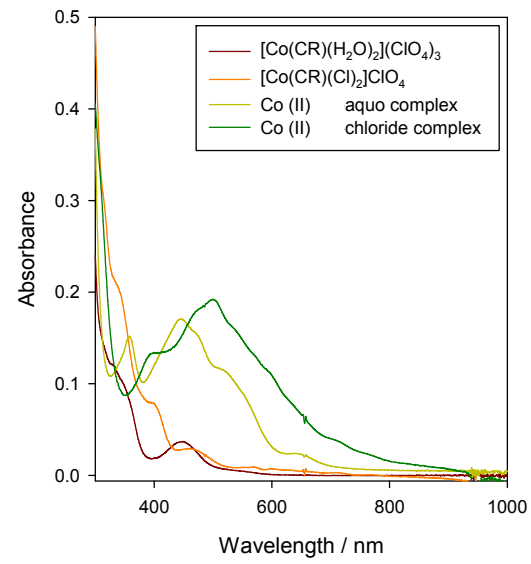


Figure S8. UV-visible absorption spectra in $\text{CH}_3\text{CN} + 0.1 \text{ M Bu}_4\text{NClO}_4$ of a 1 mM solutions of $[\text{Co}^{\text{III}}(\text{CR})\text{Cl}_2]^+$ (**Cat1**) (orange) and $[\text{Co}^{\text{III}}(\text{CR})(\text{H}_2\text{O})_2]^{3+}$ (red) and after exhaustive reduction of the solutions into the corresponding Co^{II} species (Optical pathlength 1 mm).

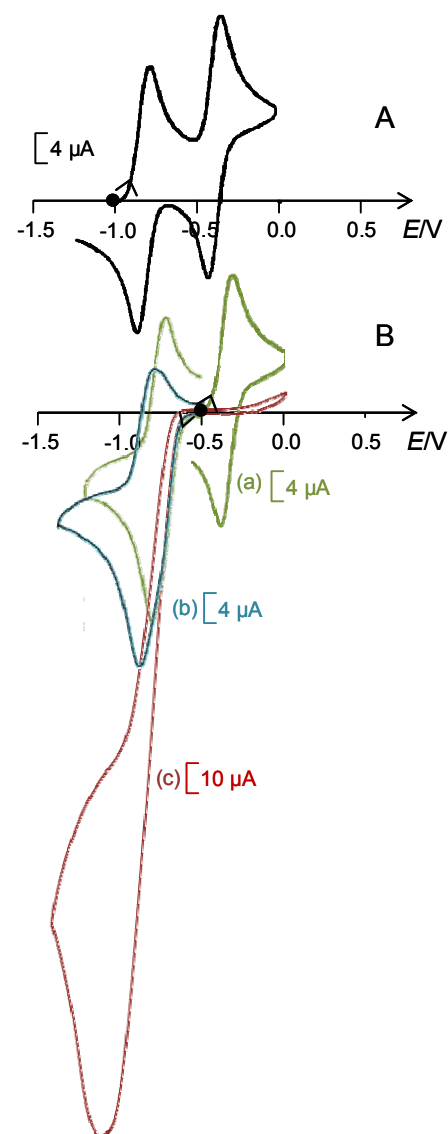


Figure S9. Cyclic voltammograms in $\text{CH}_3\text{CN} + 0.1 \text{ M } \text{Bu}_4\text{NClO}_4$ at a glassy carbon electrode ($v = 100 \text{ mV s}^{-1}$) of an electrogenerated 1 mM solution of $[\text{Co}^{\text{I}}(\text{CR})]^+$ obtained by exhaustive reduction at -1.10 V of $[\text{Co}^{\text{III}}(\text{CR})\text{Cl}_2]^+$ (Cat 1) (A) and after addition of *p*-cyano-anilinium (B): 1 equivalent (a) or 2 equivalents (b) or 20 equivalents (c).

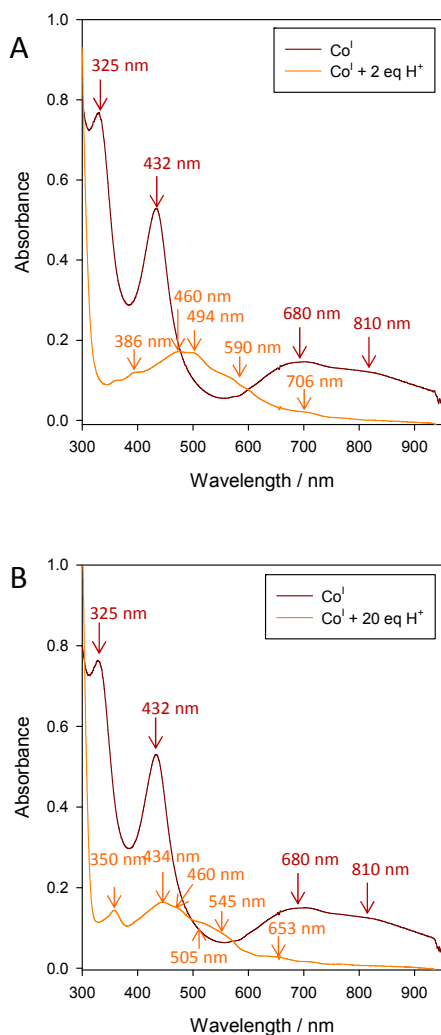


Figure S10. UV-visible absorption spectra in $\text{CH}_3\text{CN} + 0.1 \text{ M Bu}_4\text{NClO}_4$ of an electrogenerated 1 mM solution of Co^{I} from a two-electron reduction of $[\text{Co}^{\text{III}}(\text{CR})\text{Cl}_2]^+$ before (red) and after addition of p -cyano-anilinium tetrafluoroborate (orange): (A) 2 equivalents or (B) 20 equivalents, optical pathlength 1 mm.

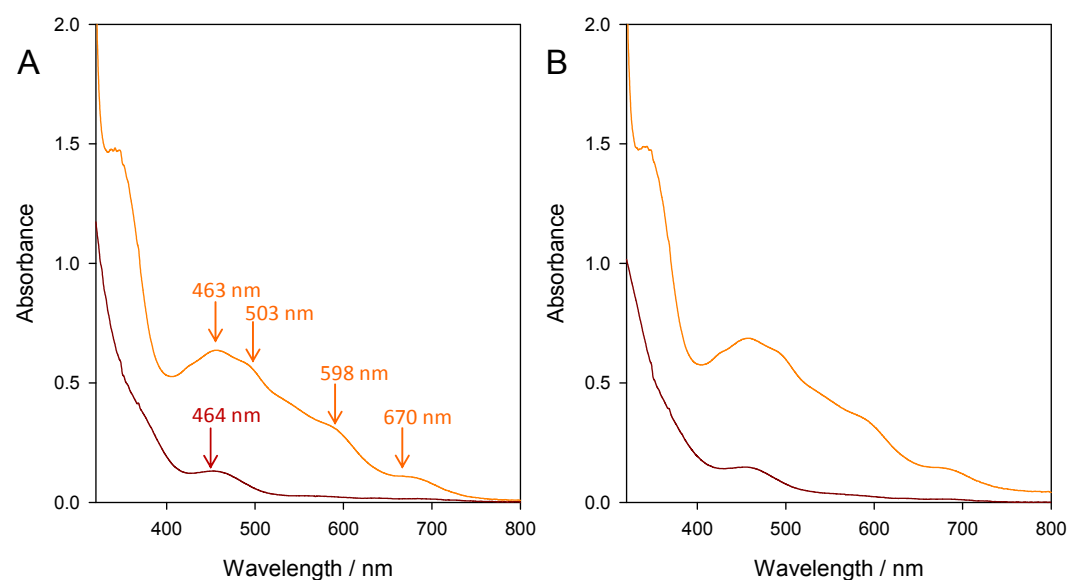


Figure S11. UV-visible absorption spectra in H_2O of a 0.35 mM solution of (A) $[\text{Co}^{\text{III}}(\text{CR})\text{Cl}_2](\text{ClO}_4)$, and (B) $[\text{Co}^{\text{III}}(\text{CR})(\text{H}_2\text{O})_2](\text{ClO}_4)_3$, initially (red) and after addition of $\text{HA}^-/\text{H}_2\text{A}$ buffer (0.55 M/0.55 M), $\text{pH} = 4.0$ (orange), optical pathlength 1 cm.

Stern-Volmer for the quenching of PS1* by $[\text{Co}^{\text{II}}(\text{CR})(\text{H}_2\text{O})_x]^{2+}$ ($x = 1$ or 2): the Stern-Volmer experiments were carried out with a deaerated aqueous solution (0.1 M acetate buffer at pH 4.0) containing **PS1** (0.01 mM) in presence of $[\text{Co}^{\text{II}}(\text{CR})(\text{H}_2\text{O})_x]^{2+}$ ($x = 1$ or 2) at different concentrations (0; 0.06; 0.08; 0.1; 0.2; 0.3 mM). These solutions were prepared by diluting an aqueous solution of $[\text{Co}^{\text{II}}(\text{CR})(\text{H}_2\text{O})_x]^{2+}$ at 0.5 mM containing 0.1 M NaClO₄ (pH 5.5), which has been obtained by an exhaustive electrolysis at $E = -0.2$ V vs Ag/AgCl of **Cat1**. Emission spectra of **PS1** in presence of $[\text{Co}^{\text{II}}(\text{CR})(\text{H}_2\text{O})_x]^{2+}$ were recorded on a Fluoromax-4 spectrofluorimeter (Horiba Scientific) at room temperature with a 1 cm path length quartz cuvette. The integrated area of the emission band of **PS1*** at 610 nm were used to calculate the I_0/I value to trace the Stern Volmer plot; I_0 is the area of the emission band of **PS1*** alone, and I is the area of the emission band of **PS1*** in presence of $[\text{Co}^{\text{II}}(\text{CR})(\text{H}_2\text{O})_x]^{2+}$. The quenching of **PS1*** by $[\text{Co}^{\text{II}}(\text{CR})(\text{H}_2\text{O})_x]^{2+}$ was estimated to be $5.1 \times 10^9 \text{ M}^{-1} \text{ s}^{-1}$.

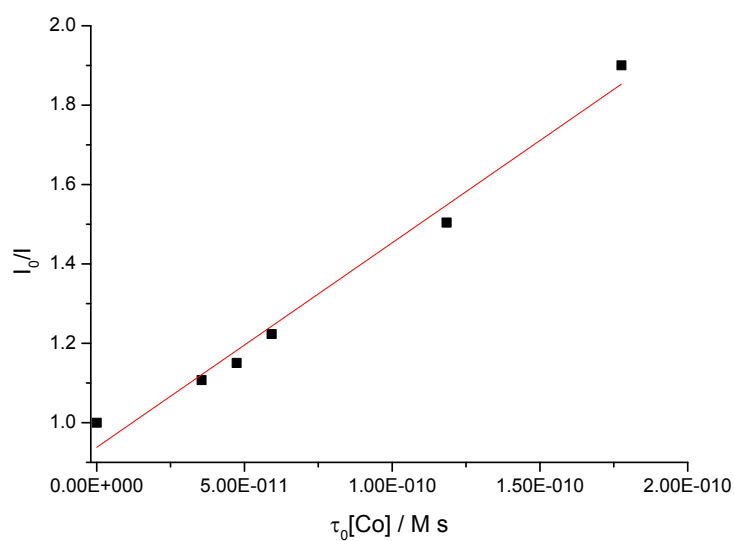


Figure S12. Stern–Volmer plot for the quenching of **PS1*** by $[\text{Co}^{\text{II}}(\text{CR})(\text{H}_2\text{O})_x]^{2+}$ in water at pH 4.0 (0.1 M acetate buffer), by varying the concentration of $[\text{Co}^{\text{II}}(\text{CR})(\text{H}_2\text{O})_x]^{2+}$ between 0 and 0.3 mM, with a concentration of **PS1** of 0.01 mM. The lifetime of **PS1*** without $[\text{Co}^{\text{II}}(\text{CR})(\text{H}_2\text{O})_x]^{2+}$ (τ_0) was determined to be 592 ns in water at pH 4.0.

References

- (1) Anton, D. R.; Crabtree, R. H. *Organometallics* **1983**, *2*, 855-859.
- (2) Paklepa, P.; Woroniecki, J.; Wrona, P. K. *J. Electroanal. Chem.* **2001**, *498*, 181-191.
- (3) Leung, C. F.; Chen, Y. Z.; Yu, H. Q.; Yiu, S. M.; Ko, C. C.; Lau, T. C. *Int. J. Hydrogen Energy* **2011**, *36*, 11640-11645.
- (4) Krishnan, C. V.; Brunschwig, B. S.; Creutz, C.; Sutin, N. *J. Am. Chem. Soc.* **1985**, *107*, 2005-2015.
- (5) Zhang, P.; Jacques, P. A.; Chavarot-Keridou, M.; Wang, M.; Sun, L. C.; Fontecave, M.; Artero, V. *Inorg. Chem.* **2012**, *51*, 2115-2120.
- (6) Stoll, T.; Gennari, M.; Serrano, I.; Fortage, J.; Chauvin, J.; Odobel, F.; Rebarz, M.; Poizat, O.; Sliwa, M.; Deronzier, A.; Collomb, M.-N. *Chem. Eur. J.* **2013**, *19*, 782-792.
- (7) Juris, A.; Balzani, V.; Barigelletti, F.; Campagna, S.; Belser, P.; Von Zelewsky, A. *Coord. Chem. Rev.* **1988**, *84*, 85-277.
- (8) Kirch, M.; Lehn, J. M.; Sauvage, J. P. *Helv. Chim. Acta* **1979**, *62*, 1345-1384.
- (9) Sivanesan, A.; John, S. A. *Biosensors & Bioelectronics* **2007**, *23*, 708-713.